Biomaterials Science

PAPER

Polysaccharide electrospun fibers with sulfated poly(fucose) promote endothelial cell migration and VEGF-mediated angiogenesis†

Cite this: DOI: 10.1039/c3bm60245a

Pim-On Rujitanaroj,‡[a] Rachida Aid-Launais,‡[b] Sing Yian Chew*[a] and Catherine Le Visage*[b,c]

Received 14th October 2013,
Accepted 12th December 2013

DOI: 10.1039/c3bm60245a

www.rsc.org/biomaterialsscience

Vascularization of tissue-engineered constructs is critical for proper cell and graft survival. In order to achieve this, pro-angiogenic factors, such as vascular endothelial growth factor (VEGF), are often incorporated into scaffolds by methods that either involve multiple steps or risk compromising protein bioactivity. In this study, we demonstrate a simple approach to incorporate VEGF into polysaccharide electrospun fibers by taking advantage of the interactions between VEGF and sulfated polysaccharide, fucoidan. Pullulan/dextran (P/D) electrospun fibers (diameter ~500 nm) incorporating fucoidan were fabricated by a one-step electrospinning process. Thereafter, VEGF was loaded onto the scaffolds. By varying the content of the chemical crosslinker, trisodium trimetaphosphate (STMP), from 10 to 12 and 16 wt% (denoted as STMP10, 12 and 16 respectively), the extent of fucoidan incorporation was significantly enhanced (<2.5 mg g^{-1} for STMP10 *vs.* 5 mg g^{-1} for STMP12 and 16). In addition, increased fucoidan content resulted in prolonged retention of VEGF bioactivity (≥14 days for STMP12 and 16 *vs.* 3 days for STMP10 and 1 day for VEGF by bolus delivery). Subcutaneous implantation of P/D scaffolds in mice demonstrated enhanced angiogenic response towards fucoidan and VEGF loaded scaffolds at 14 days post-implantation. In addition, P/D constructs supported rapid cellular infiltration and complete biodegradation of the scaffolds was observed at 7 days post-implantation. Taken together, the results demonstrate the potential of P/D electrospun fibers endowed with fucoidan as tunable reservoirs for the effective delivery of VEGF to control vascularization of tissue-engineered constructs.

1. Introduction

Vascularization is critical for proper tissue regeneration since blood vessels provide the necessary transport of nutrients, oxygen and clearance of metabolic wastes. In order to achieve proper revascularization, angiogenic factors are often used. Unfortunately, the short half-lives of these growth factors (~50 min for vascular endothelial growth factor, VEGF[1]) have often prompted the use of high dosages for systemic deliveries. Such an approach often results in unwanted side effects. In the case of VEGF, vasodilation, hypertension, inappropriate blood vessel growth and neovascularization of tumors have been seen.[1] Therefore, controlled release systems have been widely explored for the localized delivery of growth factors at therapeutic concentrations, while minimizing systemic side effects.

Besides the need for controlled and localized delivery, providing appropriate supporting structures or an extracellular matrix (ECM) to stabilize the formed vessels is also important.[2] In particular, electrospun fiber substrates appear to be promising due to their biomimicking architecture. The fact that the natural ECM consists of fibers in the sub-micron to nanometer regime highlights the relevance and importance of including these features in the design of tissue engineered constructs. Indeed, drug encapsulation,[3–6] entrapment[7] or covalent binding[8,9] onto electrospun scaffolds for tissue revascularization purposes has been explored. Although such drug incorporation methods have led to more predictable and controllable drug release, these approaches tend to involve multiple steps during scaffold fabrication and generally compromise protein bioactivity.

In this study, we demonstrate a convenient and straightforward approach to incorporating VEGF into electrospun

[a]Nanyang Technological University, School of Chemical & Biomedical Engineering, 62 Nanyang Drive, Singapore 637459, Singapore. E-mail: sychew@ntu.edu.sg
[b]Inserm, U698, Cardiovascular Bioengineering, CHU X. Bichat, 46, Rue Henri Huchard, Paris, Cedex 18 75877, France. E-mail: catherine.levisage@inserm.fr
[c]Institut Galilée, Université Paris 13, Sorbonne Paris Cité, Villetaneuse, 93430, France

†Electronic supplementary information (ESI) available. See DOI: 10.1039/c3bm60245a

‡Equal contributors.

scaffolds. Pullulan/dextran (P/D) electrospun fibers endowed with fucoidan were fabricated by a one-step electrospinning process. Following this, VEGF was incorporated into the pre-fabricated scaffolds.

Pullulan and dextran are naturally derived polysaccharides that are widely used in the pharmaceutical and biomedical industries due to their high abundance, low cost, biocompatibility and biodegradability.[10,11] Being biochemically similar to the natural ECM, these polysaccharides are also used as biodegradable scaffolds for tissue engineering.[12–15] Tubular-shaped P/D hydrogels can recapitulate the mechanical properties of a blood vessel. Their hydrophilic non-fouling surface property allows these constructs to serve as small diameter artery replacements.[15] On the other hand, P/D electrospun fibers significantly enhanced cell adhesion as compared to hydrogels[14] and maintained endothelial cell phenotype for at least 15 days *in vitro*.[13]

Fucoidan is a sulfated polysaccharide that is derived from brown seaweeds. Besides its anti-tumor, anti-inflammatory properties,[16,17] fucoidan treatment promoted neovascularization and angiogenesis and mobilized endothelial progenitor cells (EPC) *in vivo*.[18] Additionally, due to its negative sulfate groups, fucoidan binds and modulates the activity of growth factors such as VEGF.[17,19] We have previously studied *in vitro* direct interactions between VEGF and fucoidan using surface plasmon resonance and determined their binding affinity to be in the nanomolar range (K_D of 1.1×10^{-9} M).[20] We have also demonstrated that fucoidan loaded scaffolds promoted EPC proliferation. In particular, medium molecular weight (M_w = 39 kDa) fucoidan significantly potentiated VEGF angiogenic activity through its enhanced immobilization and delayed release as compared to scaffolds without fucoidans or loaded with high (600 kDa) and low (8.3 kDa) M_w fucoidans.[20] Here, we hypothesize that fucoidan may be incorporated directly into P/D electrospun fibers by electrospinning. Such electrospun fibers would possess better binding affinity for VEGF, thereby enabling the sustained and prolonged delivery of VEGF for effective angiogenesis.

2. Materials and methods

Pullulan (M_w 200 000) was purchased from Hayashibara Inc., Japan. Dextran (M_w 500 000), fucoidan (M_w 23 kDa), trisodium trimetaphosphate (STMP), gelatin, sodium hydroxide (NaOH), dimethylformamide (DMF), bovine serum albumin (BSA), fibronectin, haematoxylin, eosin, alcian blue and nuclear fast red were purchased from Sigma-Aldrich, USA and used without any further treatment. Human umbilical vein endothelial cells (HUVECs), EGM-2 Bulletkit, and endothelial basal medium-2 (EBM2) were purchased from Lonza. Vascular endothelial growth factor (VEGF) and VEGF DuoSet® ELISA Development kit were purchased from R&D Systems, USA. Fetal bovine serum (FBS) was obtained from Hyclone, USA. Phosphate-buffered saline (PBS, pH 7.4) and 40,6-diamidino-2-phenylindole (DAPI) were obtained from Gibco, Invitrogen, USA. Adult female C57/Blk mice (8 week) were obtained from Janvier, France. Ketamine (Imalgène®500) was obtained from Merial, France and xylazine (Rompun®) was obtained from Bayer HealthCare, France.

2.1. Electrospinning of pullulan/dextran and fucoidan-loaded pullulan/dextran electrospun fibers

Pullulan/dextran (P/D) electrospun fibers were fabricated according to our previous protocol.[14] Briefly, pullulan, dextran and gelatin were dissolved in a weight ratio of 8 : 2 : 1 in deionized water at room temperature at a concentration of 25 wt%. Fucoidan was added into the polymer solution at a concentration of 10 wt% of P/D and mixed overnight. Thereafter, STMP was added into the resulting solution at concentrations of 10, 12 and 16 wt% of P/D and vortexed for 2 h. The resulting solution was then mixed with DMF in a volume ratio of 10 : 1 (polysaccharide solution–DMF). Before electrospinning, 10 wt% NaOH aqueous solution was added in a volume ratio of 1 : 10 (NaOH–polysaccharide solution) to provide an alkaline condition to activate cross-linking. The resulting mixture was then transferred into a syringe and dispensed using a syringe pump (New Era Pump, USA) at a flow rate of 3.0 mL h^{-1} through a 22G needle and charged at +18 kV (GAMMA high voltage research, USA) for electrospinning. A rotating target (200 rpm) charged at −4 kV was placed 12 cm away from the needle tip. Thereafter, all scaffolds were dried at 37 °C for 7 days, followed by washing three times with DI water to remove any residual NaOH and uncrosslinked polymers. Finally, the scaffolds were cut into 12.5 mm diameter round pieces, lyophilized and stored at room temperature until further use. Table 1 summarizes the samples and their chemical content along with their notations and processing parameters.

2.2. Evaluation of scaffold morphology

Electrospun meshes were sputter coated with platinum (Pt) and evaluated by scanning electron microscopy (SEM) (JOEL, JSM-6390LA, Japan). The average fiber diameters were determined using Image J (NIH, USA) by measuring 100 fibers per sample.

Table 1 Processing parameter for electrospun scaffolds

Samples	Polymer concentration (wt%)	Fucoidan content (wt%)	STMP content (wt%)	Processing parameters
Fibers without fucoidan				
STMP10	25	0	10	
STMP12	25	0	12	+18/−4 kV
STMP16	25	0	16	3.0 mL h^{-1}
Fibers with fucoidan				
STMP10 + F	25	10	10	12 cm
STMP12 + F	25	10	12	200 rpm
STMP16 + F	25	10	16	

2.3. Phosphorus quantification

The phosphorus content of fibrous scaffolds was determined according to a colorimetric method mentioned in our previous publication.[14] About 2 mg of each scaffold were degraded with 1 mL of 10% nitric acid and incubated at 105 °C for 3 hours. Subsequently, 0.4 mL of 14.7 M nitric acid, 2 mL of 10 mM ammonium metavanadate, and 2 mL of 40 μM ammonium pentaphosphoric acid molybdate were added into each sample. For the standard curve, phosphoric acid was used as the reference and phosphorus content was then determined spectrometrically at 405 nm wavelength. Results were expressed as μmol g^{-1} dried scaffold and three scaffolds were tested for each sample.

2.4. Sulfate and fucoidan quantification

Q3 Sulfate quantification was conducted according to Gustaffson.[14] Briefly, about 30 mg of each type of scaffold was dried overnight at 60 °C. Subsequently, each sample was exposed to nitrogen (100 mL min^{-1}) while boiled in iodohydric acid for 20 minutes. Released hydrogen sulfur reacted with zinc acetate (0.2 M) to form zinc sulfur. Thereafter, 8 mL of ammonium iron sulfate (16 mM) and 2 mL of 3.7 mM diamine were added into each sample. Following 15 minutes of agitation, absorbance at 665 nm was measured using a spectrophotometer. Sulfate content was calculated from a standard curve obtained with a potassium sulfate reference solution. Sulfate content of dry fucoidan was measured and fucoidan content of all scaffolds was then calculated. At least four replicates were used for each type of scaffold.

2.5. VEGF loading and release

VEGF was reconstituted in 0.5 wt% BSA in PBS to obtain 10 μg mL^{-1}. VEGF loading onto P/D scaffolds was performed by adding 5 μL of VEGF solution (corresponding 50 ng) onto each type of dried scaffolds (average weight = 5 ± 0.25 mg). VEGF-loaded scaffolds were used for further studies. For VEGF release kinetics studies, we followed our published protocols with slight modifications.[6,21] Briefly, each scaffold was placed in a 12-well plate with 1 mL of PBS and incubated at 37 °C. At fixed time points, 500 μL of supernatant was retrieved and replenished with 500 μL of fresh PBS. The amount of released VEGF was quantified by a VEGF DuoSet® ELISA Development kit. The cumulative VEGF released (%, with respect to theoretical loading amount) was finally computed using the following equation, where the theoretical loading amount was 50 ng:

$$\text{Cumulative VEGF release} = \frac{\text{Cumulative VEGF amount (ng)}}{\text{Theoretical loading amount (ng)}} \times 100$$

2.6. Cell culture of HUVECs

HUVECs were cultured in the complete growth medium, EGM-2 Bullet kit. Cells were maintained in a humidified incubator at 37 °C with 5% CO_2. The HUVECs were kept within passages 4–10 to ensure similar cellular activity for the migration assay.

2.7. Migration assay

Transwell inserts (8 μm pores, BD Flacon, USA) were coated with 200 μL of fibronectin at 50 μg mL^{-1} concentration and incubated at 37 °C overnight. Any excessive liquid was carefully aspirated. The inserts were then washed once with PBS and dried in the hood. Scaffolds were placed in a 12-well culture plate containing 1 mL of EBM2 with 0.2% FBS and incubated at 37 °C. At specific time points, HUVECs were seeded into the inserts in 500 μL of EBM2 with 0.2% FBS and the inserts were placed in the 12-well culture plate. After 5 h, non-migratory cells were removed from the inserts by wiping the upper surface with an absorbent tip. The lower part of the inserts, containing migrated cells, was cut off and the cells were stained with DAPI (1 : 1000). Five different representative fields per insert were visualized by fluorescent microscopy (Olympus, model no. IX7) under 20× magnification. The number of nuclei was counted on three inserts for each sample group. Finally, the results were presented as migrated cells per fields.

2.8. Animal study: *in vivo* neovessels formation and scaffold degradation

The animal protocol was approved by the Bichat University Institutional Animal Care and Use Committee. Eighteen adult female C57/Blk mice (8 weeks, from Janvier, CERJ, Laval, France) were anesthetized with 2 mL of anesthetic solution (83.3 mg mL^{-1} ketamine and 3.3 mg mL^{-1} xylazine) diluted in 8 mL of distilled water (100 μL per 10 g, i.p.). Control (STMP16) and fucoidan (STMP16 + F) electrospun fiber discs of 4 mm diameter were sterilized using ultraviolet light and then hydrated extemporaneously with either PBS (5 μL) or VEGF (100 ng in 5 μl). Disc implantation was performed in the subcutaneous space of the left and right sides of the back of the mice (n = 3 discs per group).

Animals were euthanized by an overdose of ketamine/xylazine solution at day 7 or day 14 after implantation. Tissue surrounding the implantation area was harvested, fixed in 4% paraformaldehyde and embedded in OCT for histology studies. Three sections (8 μm) were cut every 100 to 150 microns in each sample and were transferred to glass slides. Hematoxylin and eosin stained sections were observed by light microscopy using the NDPview software (Hamamatsu, Japan) and the number of blood vessels was evaluated and expressed in number per mm^2 as previously reported.[20] At least 3 sections of each sample were used for quantification, taken at different depths of the harvested tissues (Table 2). Q4

In a separate experiment, STMP16 scaffolds were implanted and animals were sacrificed at day 1, day 4 and day 7. Tissue sections were stained with alcian blue and nuclear fast red to assess the scaffold degradation following implantation. Scaffold area was measured on histology sections using NDPview software (Hamamatsu, Japan) and expressed in mm^2.

Table 2 Subcutaneous study design. A total of 24 samples were implanted into 12 mice; an additional study was performed with 6 mice to assess the *in vivo* fate of the polysaccharide scaffold (2 mice were sacrificed at each time point)

Samples	Day 1	Day 4	Day 7	Day 14
STMP16	—	—	$n = 3$	$n = 3$
STMP16 + F	—	—	$n = 3$	$n = 3$
STMP16 + VEGF	—	—	$n = 3$	$n = 3$
STMP16 + F + VEGF	—	—	$n = 3$	$n = 3$
STMP16	$n = 3$	$n = 3$	$n = 3$	—

2.9. Statistics

Fiber diameters are expressed as mean ± standard deviation. All other results are expressed as mean ± standard error (SE) of mean. Phosphorus content, sulfate content, fucoidan content and cell migration were analyzed using one-way ANOVA and Tukey's *post doc* test for more than two sample groups after verifying equal variances; otherwise, non-parametric tests, Kruskal–Wallis and Mann–Whitney *U* tests, were used. Student's *t*-test was used for statistical comparisons involving two samples. Blood vessel density results were analyzed using a two-way ANOVA with Bonferroni's *post hoc* test. Scaffold area results were analyzed using a one-way ANOVA with Bonferroni's *post hoc* test. Values of $p < 0.05$ were considered statistically significant.

3. Results

3.1. Scaffold morphology

As indicated in Fig. 1(A–C), fucoidan-loaded P/D scaffolds with uniform and bead-free fibers were obtained. The average diameters of as-spun fucoidan-loaded P/D fibers with different loading concentrations of 10 wt%, 12 wt% and 16 wt% STMP were 489 ± 145 nm, 508 ± 161 nm and 513 ± 158 nm respectively. No significant increase in fiber diameter was observed with increasing STMP content. After washing and drying, the scaffolds retained the porous and fibrous architectures as indicated in Fig. 1(D–F).

3.2. Phosphorus content

In this study, STMP was used as a chemical crosslinking agent for polysaccharide-based electrospun fibers. The crosslinking is a result of phosphate bridge formation between polymer chains.[15] Therefore, phosphorus content was used as an estimate of the crosslinking efficacy between the polymer chains. Fig. 2 shows that the amount of phosphorus in fibers without fucoidan significantly increased with STMP concentration (384 ± 8.5 μmol g^{-1}, 578 ± 40.5 μmol g^{-1}, and 932 ± 86.6 μmol g^{-1} for STMP10, STMP12 and STMP16, respectively, $p < 0.05$). The

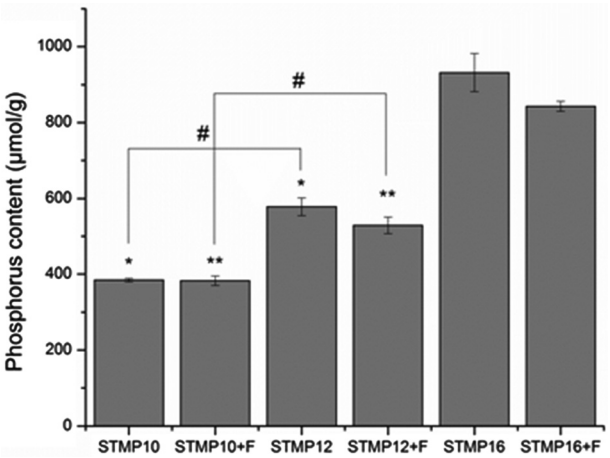

Fig. 2 Phosphorus content of cross-linked scaffolds as determined by the colorimetric test. * and ** indicate $p < 0.05$ as compared to STMP16 and STMP16 + F respectively. # indicates $p < 0.05$. Results are presented as mean values ± SE ($n = 3$).

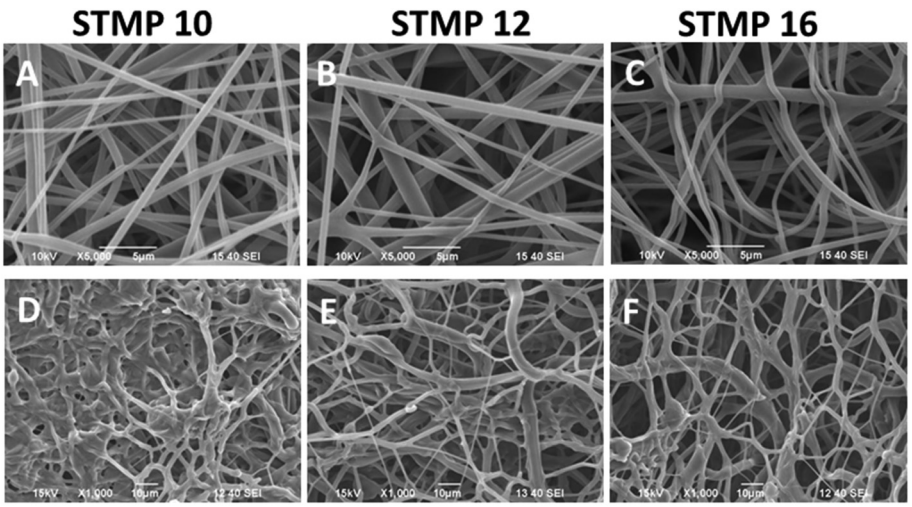

Fig. 1 SEM images of (A–C) as-spun fucoidan-loaded pullulan/dextran fibers and (D–F) fucoidan-loaded pullulan/dextran fibers after washing and drying. Results indicate the retention of scaffold fibrous architecture.

addition of 10 wt% of fucoidan did not impair the crosslinking process since the scaffolds presented similar phosphorus contents at each STMP concentration.

3.3. Sulfate and fucoidan content

Incorporation of sulfated fucoidan into electrospun scaffolds was then evaluated with the measurement of sulfate content. As indicated in Fig. 3, sulfate content significantly increased with the incorporation of STMP (6 ± 1 μmol g^{-1}, 20 ± 4 μmol g^{-1}, and 16 ± 2 μmol g^{-1} for STMP10 + F, STMP12 + F and STMP16 + F, respectively, $p < 0.05$). However, there was no significant increase in sulfate content between STMP12 + F and STMP16 + F, likely due to the saturation of fucoidan that could be entrapped in the electrospun fibers. Fucoidan content of scaffolds was then calculated based on their respective fucoidan sulfate content. A similar trend was observed for fucoidan content (Fig. 3).

3.4. Release kinetics of VEGF-loaded scaffolds

Fig. 4 shows the release profiles of VEGF from electrospun scaffolds. A sustained release of VEGF was detected for up to 7 days after initial burst releases upon immersion into PBS. The encapsulation of fucoidan within P/D electrospun fibers resulted in a significantly lower burst release than plain electrospun scaffolds (19.3 ± 0.5% (STMP10 + F), 16.2 ± 1.1% (STMP12 + F), 15.3 ± 0.6% (STMP16 + F) *vs.* 20.9 ± 0.6% (STMP16), at $t = 5$ h, $p < 0.05$). The increase in cross-linker concentration appeared to slow the initial burst release of VEGF from electrospun fibers, although the difference was not statistically significant for STMP12 + F and STMP16 + F. Concurrently, the rate and amount of VEGF that was released from fucoidan-loaded scaffolds were lower as compared to plain electrospun fibers. At day 14, the total cumulative release of VEGF was 22.8 ± 1.0%, 23.7 ± 0.2%, and 24.2 ± 0.5% for STMP10 + F, STMP12 + F and STMP16 + F, respectively and a significantly higher release of 29.2 ± 0.1% was detected from plain electrospun fibers ($p < 0.05$). These results suggested that fucoidan helped to retain VEGF throughout the period of sustained release.

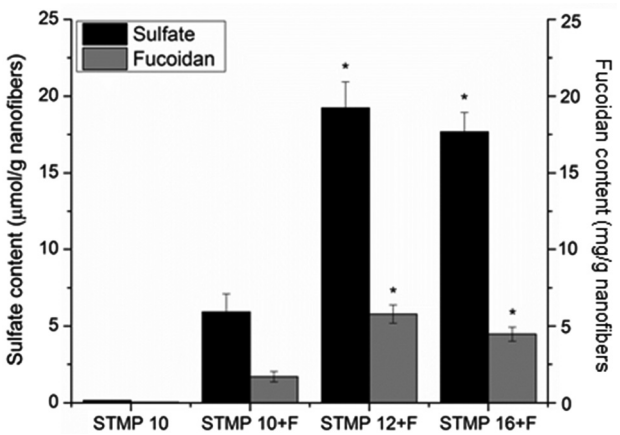

Fig. 3 Sulfate content of scaffolds with and without incorporation of fucoidan as measured following reduction by hydriodic acid. Scaffolds without fucoidan were used as controls. Fucoidan content of scaffolds was then calculated from the corresponding fucoidan fraction sulfate content. * indicates a significant difference with STMP10 + F scaffolds ($p < 0.05$). Results are presented as mean values ± SE ($n = 3$).

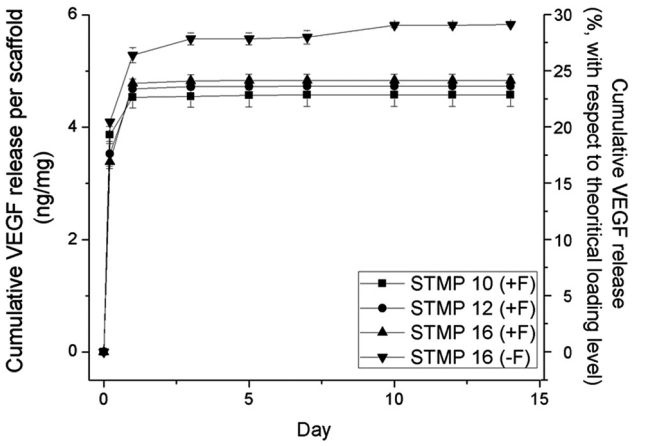

Fig. 4 VEGF cumulative release from scaffolds with and without incorporation of fucoidan. VEGF release was measured by ELISA after specific time points of incubation in PBS at 37 °C. $n = 4$.

3.5. Bioactivity of VEGF released from scaffolds

A migration assay of HUVECs was performed in order to investigate the bioactivity of VEGF released from electrospun scaffolds. As shown in Fig. 5 and ESI Fig. 1,† bolus delivery of VEGF resulted in a significantly higher number of migrated cells than VEGF-loaded fucoidan scaffolds at day 1 ($p < 0.05$). However, the number of migrated cells in response to bolus VEGF decreased significantly by day 3 and returned to the basal level after 7 days. Meanwhile, the difference in cell migration was not statistically significant for scaffolds with fucoidan alone as compared to untreated cells at all time points (ESI Fig. 2†). For VEGF-loaded fucoidan scaffolds, higher STMP concentration demonstrated lower cell migration at day 1 (migrated cells: STMP16 + F ≈ STMP12 + F < STMP10 + F, $p < 0.05$), likely due to the lower initial burst release of VEGF from the scaffolds. Although the number of migrated cells for STMP12 + F and STMP16 + F samples was significantly lower at the initial time point, the number of migrated cells was significantly higher as compared to bolus delivery from day 5 to day 14. This is likely due to the sustained release and availability of VEGF from fucoidan electrospun fibers. This observation contrasted with trends observed on STMP10 + F, where the number of migrated cells returned to basal level after 7 days.

3.6. Animal study

Since *in vitro* results revealed better VEGF release from P/D electrospun fibers that were crosslinked with 16 wt% of STMP, these scaffolds were used in subsequent *in vivo* studies. In the first series of experiments, control (STMP16) and fucoidan (STMP16 + F) electrospun fibers were hydrated extemporaneously with either PBS (5 μL) or VEGF (100 ng in 5 μl) and

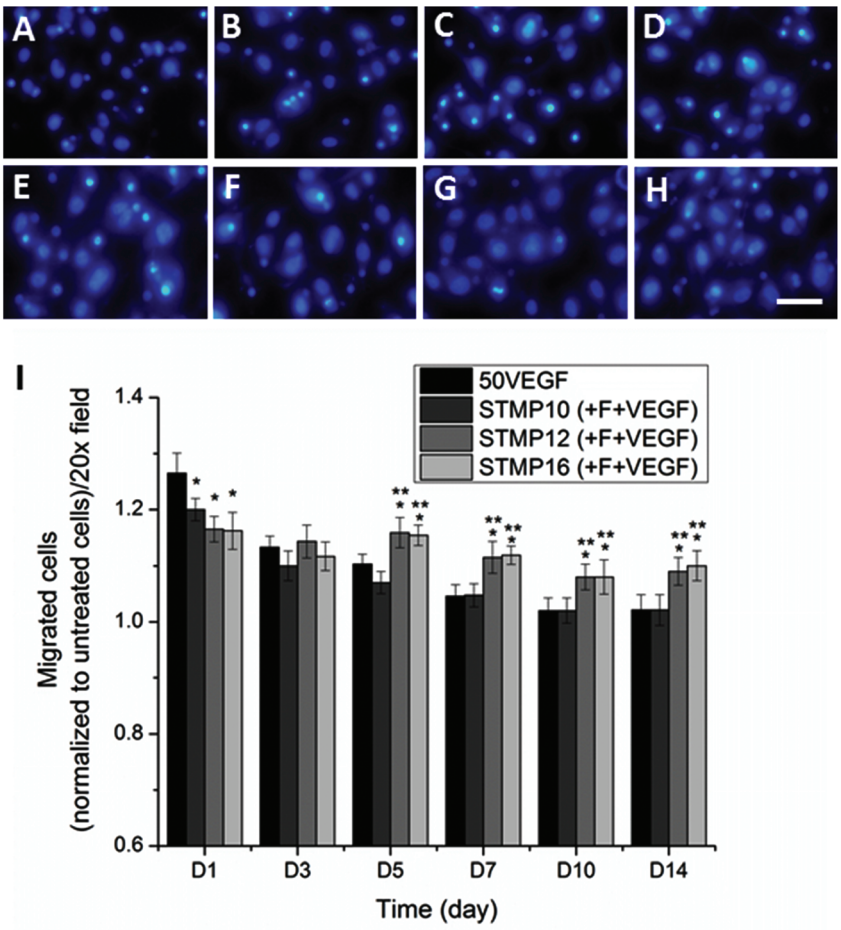

Fig. 5 Migration of HUVECs in a transwell chemotaxis assay (n = 3, transwells). Representative images (A)–(H) of migrated HUVECs at day 14. Blue signals present cell nuclei by DAPI staining. The scale bar is 50 μm. (A) and (E) With and without bolus delivery of 50 ng mL^{-1} VEGF respectively. (B)–(D) Fucoidan scaffolds with STMP10, STMP12 and STMP16 respectively. (F)–(H) VEGF-loaded fucoidan scaffolds with STMP10, STMP12 and STMP16 respectively. (I) Quantitative analysis of migrated cells. * and ** indicate $p < 0.05$ as compared to samples with bolus delivery of VEGF and STMP10 (+F + VEGF) samples at each time point respectively.

then implanted in a subcutaneous angiogenesis model in mice. Fig. 6a shows representative images of haematoxylin/eosin stained tissue sections harvested at day 14. Similar to day 7 (not shown), macroscopic observation evidenced a complete disappearance of the scaffolds in all groups. In the presence of fucoidan and VEGF (STMP16 + F + VEGF scaffolds), a more intense vascularization response was observed. Furthermore, the increased presence of erythrocytes demonstrated the functionality of the neoformed blood vessels (black arrows). As indicated in Fig. 6b, there was a significant difference in blood vessel density between the STMP16 + F + VEGF scaffold and all other groups at day 7 ($p < 0.01$ for STMP16, $p < 0.001$ for STMP16 + F and $p < 0.05$ for STMP16 + VEGF) and at day 14 ($p < 0.001$ for all cases).

In the second set of experiments, electrospun fibers were implanted subcutaneously in mice to assess the *in vivo* fate of the polysaccharide scaffold. At day 1, samples were retrieved and scaffolds, as well as the electrospun fiber structure, were clearly identified on alcian blue stained histology sections (Fig. 6D). At day 4, we noticed that the scaffold had shrunk. In addition, cellular infiltration, as illustrated with an insert from day 4 image, was evident with red stained cells located in-between the loose electrospun fibers. At day 7, there was almost no scaffold left at the site of implantation and this was confirmed with a significant decrease of the scaffold area, as measured on histology sections, from day 1 to day 4 and day 7 (2.49 ± 0.18 mm^2 *versus* 1.49 ± 0.04 mm^2 *versus* 0.004 ± 0.001 mm^2, respectively, $p < 0.01$).

4. Discussion

In this study, we incorporated polysaccharide fucoidan into electrospun pullulan–dextran fibers. Functionalized fibrous scaffolds were assessed as tunable reservoirs and delivery systems for VEGF, a potent angiogenic molecule, *in vitro* and *in vivo*.

Inadequate nutrient perfusion and mass transport issues, especially oxygen diffusion, limit the development of tissue-engineered products to smaller than clinically relevant sizes

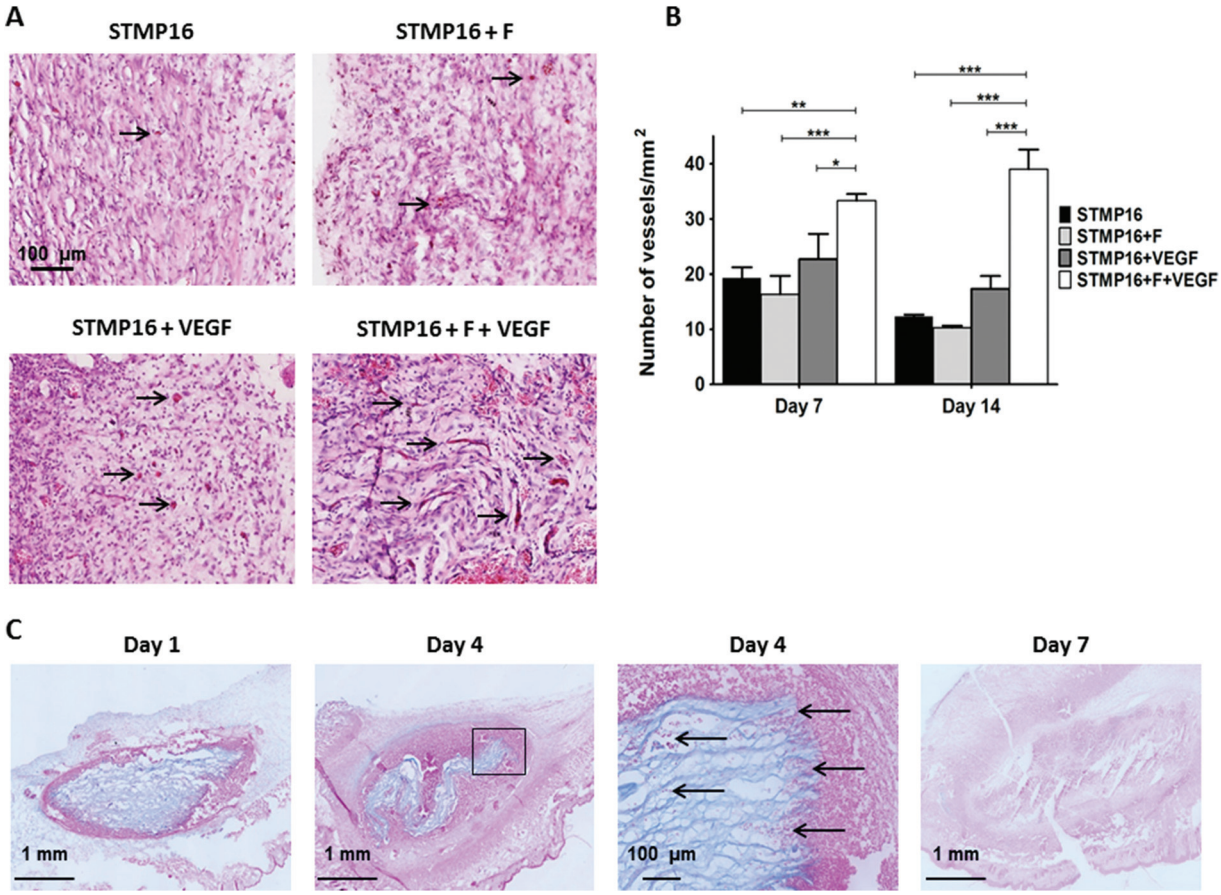

Fig. 6 (A) Following subcutaneous implantation, neovessel formation (arrows) was assessed on hematoxylin/eosin stained sections of tissues harvested two weeks after subcutaneous implantation. (B) Neovessels were quantified and results were expressed as the number of neovessels per μm^2 (*$p < 0.05$, **$p < 0.01$, ***$p < 0.001$). (C) STMP16 scaffold degradation was assessed on sections stained with alcian blue and nuclear red to visualize polysaccharide fibers and cells, respectively. At day 4, a significant decrease of the scaffold area was observed as compared to day 1, with cellular infiltration noted in-between the loose electrospun fibers (arrows). At day 7, only remnants of the fibrous scaffold could be found.

and impair their subsequent integration *in vivo*. Many cellular studies have sought to use prevascularized or endothelialized scaffolds to induce neovascularization and enhance integration with host vasculature. Another strategy relies on the use of a pro-angiogenic biomaterial that would not require any cell culture step before implantation, while providing biological cues to improve EPC recruitment.[22] Spatial and temporal presentation of these cues at the site of tissue repair would be critical for achieving proper microvascular network formation and stabilization. It is well documented that the pro-angiogenic protein, VEGF,[22] not only stimulates the proliferation and migration of endothelial cells to establish nascent microvessel but also recruits mononuclear cells and macrophages that produce additional angiogenic factors.[23] Simón-Yarza and coauthors reviewed the main drug delivery systems that have been developed to administer VEGF in cardiovascular diseases.[24] Most of these systems require covalent binding such as VEGF immobilized in poly(ethylene glycol)-diacrylate hydrogels.[25] To overcome the potential damage to VEGF and the loss of biological activity that may result from the covalent chemistry, development of growth factor-binding biomaterials has emerged as another strategy. We thus selected fucoidan, a sulfated polysaccharide, to functionalize electrospun P/D fibers into tunable VEGF reservoirs.

We previously reported the fabrication of electrospun polysaccharide fibers using STMP as a chemical cross-linker.[13,14] Polysaccharides were mixed with STMP to enable *in situ* cross-linking during the electrospinning process. In this study, STMP concentrations ranged from 10 to 16 wt% of polysaccharides. Cross-linking occurs through the formation of an intermolecular linkage between two hydroxyl groups within the polymer chains as demonstrated for pullulan.[26] Fucoidan molecules bearing hydroxyl groups might react as well with STMP thus becoming part of the hydrogel network. Indeed, when increasing the concentration of STMP from 10 to 12 wt%, an increase of fucoidan content in electrospun fibers was obtained. However, a further increase of STMP concentration to 16 wt% did not increase the fucoidan content of the fibrous scaffolds.

In a previous work, we demonstrated that both molecular weight and sulfate content influenced fucoidan incorporation into chemically cross-linked porous hydrogels.[20] A low

molecular weight (8.3 kDa) fucoidan was not efficiently cross-linked into the hydrogel framework and the resulting fucoidan content was less than 3 mg g^{-1} of scaffold. Increasing the molecular weight of fucoidan resulted in a significant increase of the fucoidan content up to 80 mg g^{-1} scaffolds, with longer chains bearing multiple hydroxyl groups more efficiently cross-linked to the pullulan and dextran framework.

Hence, based on these results, we selected in this study a medium molecular weight fucoidan, similar to the one used in our previous work. Although electrospun fibers were prepared using a higher cross-linker concentration and their phosphorus content was at least 3 times higher than in porous scaffolds, a low fucoidan content of ~5 mg g^{-1} of electrospun fibers was reached. This result indicates that either all hydroxyl groups of pullulan and dextran chains were involved in cross-linked bonds or all hydroxyl groups that were sterically available on fucoidan molecules were participating in these bonds; either way, no additional fucoidan could be incorporated.

We then demonstrated that fucoidan content was high enough to impact VEGF bioactivity on endothelial cells. Indeed, STMP10 electrospun fibers that contained less than 3 mg g^{-1} were less effective than STMP12 and STMP16 scaffolds for stimulating cell migration. In addition, both VEGF loaded STMP12 and STMP16 scaffolds that had similar fucoidan content presented similar bioactivity. One might assume that the number of sulfate groups associated with the functionalized electrospun fibers would be a more relevant parameter than the fucoidan content, since structure–function studies have reported that the distribution of negative charges of sulfate groups on the fucoidan backbone rather than its molecular weight is important for biological activities.[27] Here, we demonstrated that both VEGF loaded STMP12 and STMP16 electrospun scaffolds presented similar sulfate content and similar bioactivity, confirming a relationship between sulfate groups and biological activities of fucoidan scaffolds.

One commonly encountered problem is the difficulty in fully colonizing even relatively thin (~1 mm) electrospun scaffolds.[28] Inadequate cell infiltration occurs and limits integration with native structures when these scaffolds are implanted *in vivo*. To our surprise, following subcutaneous implantation in mice, we observed cells infiltrating in-between layers of electrospun fibers, coupled with a drastic reduction of the scaffold size within 4 days, as measured on alcian blue stained histological sections. By day 7, fibers could not be identified on tissue sections and all scaffolds had disappeared. This bioerosion timeframe is particularly striking as compared to our previous reports on P/D porous scaffolds. These 1 mm thick scaffolds, obtained by a similar STMP cross-linking process combined with a salt leaching technique, presented large interconnected pores (~200 microns). Following cardiac implantation in rat hearts, it took almost 2 months to observe a similar bioerosion of scaffolds that were 3 times less cross-linked.[29] Thus, these electrospun scaffolds could be considered as highly porous biomaterials, in which cells can quickly infiltrate in-between fiber layers. These cells would then favor the scaffold erosion through enzymatic hydrolysis of phosphoester bonds that we introduced during the cross-linking process.[30] This fast erosion rate might be finely tuned by adjusting the cross-linker content to optimize the delivery duration.

Another important finding of this study was the demonstration that a hydrogel fibrous system could be used to achieve a sustained release of biologically active VEGF following local implantation and the desired outcome of neovascularization. The approach of scaffold decoration with fucoidan probably mimics the *in vivo* conditions where growth factors are associated with the extracellular matrix through dynamic direct and indirect interactions.[31] Fucoidan had a marked positive effect on angiogenesis, suggesting that it could directly bind to and release certain growth factors, as well as sequester them and/or enhance their activity. One advantage of the fibrous system is its flexibility in terms of VEGF dose through a simple change in concentration of the solution loaded on the scaffold. In addition, one can envisage administering electrospun fibers prepared with either different fucoidan content or cross-linker content to obtain different VEGF release profiles. A local release of VEGF from the functionalized scaffold, in addition to the electrospun fiber features, could have contributed to the formation and stabilization of microvascular networks, highlighting the importance of controlling the biochemical and structural microenvironment for biomaterial-based vascularization.

5. Conclusion

In this study, we demonstrate a one-step preparation of electrospun scaffolds functionalized with non-animal sulfated polysaccharide fucoidan. We demonstrate that VEGF loaded scaffolds potentiate VEGF *in vitro* bioactivity on endothelial cells, trigger an angiogenic response following subcutaneous implantation in mice, as well as favor cellular infiltration and subsequent bioerosion of the biomaterial. Such functionalized electrospun fibers offer exciting approaches for clinical applications.

Acknowledgements

This work was supported in part by grants from MOE AcRF Tier 1 (RG 75/10), the MechanoBiology Institute (R-714-013-007-271), NMRC-CBRG (CBRG11NOV067) and University Paris 13. We are grateful to M. Maire (University Paris 13) for assistance with sulfate content measurements.

References

1 C. D. Gaudio, S. Baiguera, M. Boieri, B. Mazzanti, D. Ribatti, A. Bianco and P. Macchiarini, Induction of angiogenesis using VEGF releasing genipin-crosslinked electrospun gelatin mats, *Biomaterials*, 2013, **34**, 7754–7765.

2 Y.-D. Lin, C.-Y. Luo, Y.-N. Hu, M.-L. Yeh, Y.-C. Hsueh, M.-Y. Chang, D.-C. Tsai, J.-N. Wang, M.-J. Tang, E. I. H. Wei, M. L. Springer and P. C. H. Hsieh, Instructive nanofiber scaffolds with VEGF create a microenvironment for arteriogenesis and cardiac repair, *Sci. Transl. Med.*, 2012, **4**(146), 146ra109.

3 Z. Xie, C. B. Paras, H. Weng, P. Punnakitikashem, L.-C. Su, K. Vu, L. Tang, J. Yang and K. T. Nguyen, Dual growth factor releasing multi-functional nanofibers for wound healing, *Acta Biomater.*, 2013, In press.

4 H. Seyednejab, W. Ji, F. Yang, C. F. v. Nostrum, T. Vermonden, J. J. P. P. v. d. Beucken, W. J. A. Dhert, W. E. Hennink and J. A. Jansen, Coaxxially electrospun scaffolds based on hydroxyl-functionalized poly(epsilon-caprolactone) and loaded with VEGF for tissue engineering applications, *Biomacromolecules*, 2012, **13**, 3650–3660.

5 H. Zhang, X. Jia, F. Han, J. Zhao, Y. Zhao, Y. Fan and X. Yuan, Dual-delivery of VEGF and PDGF by double-layered electrospun membranes for blood vessel re-generation, *Biomaterials*, 2013, **34**, 2202–2212.

6 S. Y. Chew, J. Wen, E. K. F. Yim and K. W. Leong, Sustained release of proteins from electrospun biodegradable fibers, *Biomacromolecules*, 2005, **6**(4), 2017–2024.

7 A. K. Ekaputra, G. D. Prestwich, S. M. Cool and D. W. Hutmacher, The three-dimensional vascularization of growth factor-releasing hybrid scaffold of poly (epsilon-caprolactone)/collagen fibers and hyaluronic acid hydrogel, *Biomaterials*, 2011, **32**, 8108–8117.

8 F. Du, HaoWang, W. Zhao, D. Li, D. Kong, J. Yang and Y. Zhang, Gradient nanofibrous chitosan/poly epsilon-caprolactone scaffolds as extracellular microenvironments for vascular tissue engineering, *Biomaterials*, 2012, **33**, 762–770.

9 L. Ye, X. Wu, H.-Y. Duan, X. Geng, B. Chen, Y.-Q. Gu, A.-Y. Zhang, J. Zhang and Z.-G. Feng, The in vitro and in vivo biocompatibility evaluation of heparin-poly(epsilon-caprolactone) conjugate for vascular tissue engineering scaffolds, *J. Biomed. Mater. Res., Part A*, 2012, **100A**, 3251–3258.

10 I. L. Shih, Microbial exo-polysaccharides for biomedical applications, *Mini-Rev. Med. Chem.*, 2010, **10**(14), 1345–1355.

11 A. Sizovs, P. M. McLendon, S. Srinivasachari and T. M. Reineke, Carbohydrate Polymers for Nonviral Nucleic Acid Delivery, *Top. Curr. Chem.*, 2010, **296**, 131–190.

12 J. C. Fricain, S. Schlaubitz, C. L. Visage, I. Arnault, S. M. Derkaoui, R. Siadous, S. Catros, C. Lalandea, R. Bareille, M. Renard, T. Fabre, S. Cornet, M. Durand, A. Léonard, N. Sahraoui, D. Letourneur and J. Amédée, A nano-hydroxyapatite – Pullulan/dextran polysaccharide composite macroporous material for bone tissue engineering, *Biomaterials*, 2013, **34**(12), 2947–2959.

13 L. Shi, R. Aid, C. L. Visage and S. Y. Chew, Biomimicking polysaccharide nanofibers promote vascular phenotypes: A potential application for vascular tissue engineering, *Macromol. Biosci.*, 2012, **12**(3), 395–401.

14 L. Shi, C. L. Visage and S. Y. Chew, Long-Term Stabilization of Polysaccharide Electrospun Fibres by In Situ Cross-Linking, *J. Biomater. Sci., Polym. Ed.*, 2011, **22**(11), 1459–1472.

15 M. Chaouata, C. L. Visage, A. Autissier, F. Chaubet and D. Letourneur, The evaluation of a small-diameter polysaccharide-based arterial graft in rats, *Biomaterials*, 2006, **27**(32), 5546–5553.

16 W. A. J. P. Wijesinghe and Y.-J. Jeon, Biological activities and potential industrial applications of fucose rich sulfated polysaccharides and fucoidans from brown seaweeds: A review, *Carbohydr. Polym.*, 2012, **88**, 13–20.

17 K. Senthilkumar, P. Manivasagan, J. Venkatesan and S.-K. Kim, Brown seaweed fucoidan: Biological activity and apoptosis, growth signaling mechanisms in cancer, *Int. J. Biol. Macromol.*, 2013, **60**, 366–374.

18 S. Manzo-Silberman, L. Louedec, O. Meilhac, D. Letourneur, J.-B. Michel and I. Elmadbouh, Therapeutic potential of fucoidan in myocardial ischemia, *J. Cardiovasc. Pharmacol.*, 2011, **58**(6), 626–632.

19 C. Boisson-Vidal, F. Zemani, C. Caligiuri, I. Galy-Fauroux, S. Colliec-Jouault, D. Helley and A.-M. Fischer, Neoangiogenesis induced by progenitor endothelial cells: Effect of fucoidan from marine algae, *Cadiovasc. Hematol. Agents Med. Chem.*, 2007, **5**, 67–77.

20 A. Purnama, R. Aid-Launais, O. Haddad, M. Maire, D. Mantovani, D. Letourneur, H. Hlawaty and C. LeVisage, Fucoidan in a 3D scaffold interacts with vascular endothelial growth factor and promotes neovascularization in mice, *Drug Delivery Transl. Res.*, 2013, in press.

21 S. Y. Chew, R. Mi, A. Hoke and K. W. Leong, Aligned Protein–Polymer Composite Fibers Enhance Nerve Regeneration: A Potential Tissue-Engineering Platform, *Adv. Funct. Mater.*, 2007, **17**(8), 1288–1296.

22 J. W. Andrejecsk, W. G. Chang, J. S. Pober and W. M. Saltzman, Controlled protein delivery in the generation of microvascular networks, *Drug Delivery Transl. Res.*, 2012, in press.

23 M. Grunewald, I. Avraham, Y. Dor, E. Bachar-Lustig, A. Itin, S. Yung, S. Chimenti, L. Landsman, R. Abramovitch and E. Keshet, VEGF-Induced Adult Neovascularization: Recruitment, Retention, and Role of Accessory Cells, *Cell*, 2006, **124**(1), 175–189.

24 T. Simón-Yarza, F. R. Formiga, E. Tamayo, B. Pelacho, F. Prosper and M. J. Blanco-Prieto, Vascular Endothelial Growth Factor-Delivery Systems for Cardiac Repair: An Overview, *Theranostics*, 2012, **2**(6), 541–552.

25 J. E. Leslie-Barbicka, J. J. Moonb and J. L. Westc, Covalently-Immobilized Vascular Endothelial Growth Factor Promotes Endothelial Cell Tubulogenesis in Poly(ethylene glycol) Diacrylate Hydrogels, *J. Biomater. Sci., Polym. Ed.*, 2009, **20**(12), 1763–1779.

26 S. Lack, V. Dulong, D. L. Cerf, L. Picton, J. F. Argillier and G. Muller, Hydrogels Based on Pullulan Crosslinked with sodium trimetaphosphate (STMP): Rheological study, *Polym. Bull.*, 2004, **52**(6), 429–436.

27 F. Haroun-Bouhedja, M. Ellouali, C. Sinquin and C. Boisson-Vidal, Relationship between Sulfate Groups and Biological Activities of Fucans, *Thromb. Res.*, 2000, **100**(5), 453–459.

28 B. M. Baker, A. M. Handorf, L. C. Ionescu, W.-J. Li and R. L. Mauck, New directions in nanofibrous scaffolds for soft tissue engineering and regeneration, *Expert Rev. Med. Devices*, 2009, **6**(5), 515–532.

29 C. Le-Visage, O. Gournay, N. Benguirat, S. Hamidi, L. Chaussumier, N. Mougenot, J. A. Flanders, R. Isnard, J.-B. Michel, S. Hatem, D. Letourneur and F. Norol, Mesenchymal Stem Cell Delivery into Rat Infarcted Myocardium Using a Porous Polysaccharide-Based Scaffold: A Quantitative Comparison With Endocardial Injection, *Tissue Eng., Part A*, 2012, **18**(1–2), 35–44.

30 K. Manoi and S. S. H. Rizvi, Physicochemical characteristics of phosphorylated cross-linked starch produced by reactive supercritical fluid extrusion, *Carbohydr. Polym.*, 2010, **81**(3), 687–694.

31 G. S. Schultz and A. Wysocki, Interactions between extracellular matrix and growth factors in wound healing, *Wound Repair Regen.*, 2009, **17**(2), 153–162.